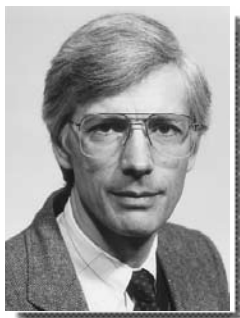


New Seismic Design Provisions for Diaphragms in Precast Concrete Parking Structures

Sharon L. Wood, Ph.D., P.E.

Professor
Department of Civil Engineering
University of Texas
Austin, Texas



John F. Stanton, Ph.D., P.E.

Professor
Department of Civil and Environmental
Engineering
University of Washington
Seattle, Washington

Neil M. Hawkins, Ph.D.

Professor
Department of Civil and Environmental
Engineering
University of Illinois
Urbana, Illinois



Diaphragm damage was observed in several precast concrete parking structures following the 1994 Northridge earthquake. In order to reduce the likelihood of damage in future earthquakes, the design provisions for chord reinforcement in diaphragms were modified in the 1997 Uniform Building Code, and new provisions for selecting web reinforcement were introduced in the 1999 ACI Building Code. This paper focuses on recent changes to the ACI Building Code and summarizes the results of a series of analyses of idealized buildings to demonstrate that diaphragms proportioned in accordance with earlier codes may be vulnerable to seismic damage. A diverse set of factors, including the orientation of precast members and the stress-strain characteristics of welded wire fabric, contributed to the observed damage in precast concrete parking structures.

Several precast concrete parking structures sustained structural damage during the 1994 Northridge earthquake.^{1,2,3} Buckled diaphragm chord reinforcement and development of cracks across the entire width of the diaphragm were the most common types of observed damage (see Figs. 1 and 2). The damage was often accompanied by shifting of precast members, and portions of the precast gravity-load-resisting systems did collapse in some structures (see Figs. 3 and 4). Engineers have hypothesized that



Fig. 1. Buckled chord reinforcement in diaphragm.



Fig. 2. Concentrated cracks along column lines.

more extensive damage could have occurred if the duration of the earthquake had been longer because more of the precast members would have become unseated.⁴

Important observations about the seismic response of precast concrete parking structures can be made based on the observed damage. The structures highlight a fundamental inconsistency in the seismic design provisions used throughout the United States. Codes relate the seismic design forces for a building to the deformation capacity of the vertical elements of the lateral-force-resisting system.

The parking structure shown in Fig. 5 demonstrates that this approach is not universally valid. It is clear that the response of this structure during the Northridge earthquake was controlled by the weakest link in the entire structural system, and not by the inelastic response of the structural walls.

A second observation is that the layout of the precast concrete members, the placement of the structural walls, and the choice of reinforcement in the diaphragms influenced the seismic response of the parking structures.^{5,6} In the epicentral region, precast concrete parking structures were typically constructed with cast-in-place topping slabs that were reinforced to act as diaphragms. Temperature effects and shrinkage led to the development of cracks in the topping slabs; therefore, the diaphragms were cracked before the earthquake. Because no precast or cast-in-place concrete members crossed the paths of these cracks, the crack widths increased in size during the earthquake (see Figs. 1 and 2).

Subsequent analyses^{5,6} have shown that the distributed reinforcement commonly used in the topping slabs did not have the strain capacity to bridge these cracks. Fracture of the web reinforcement led to significant decreases in the calculated shear strength of the diaphragms.

RESEARCH PROGRAM

The objective of this research program was to determine if precast concrete parking structures were more susceptible to earthquake damage than other types of structural concrete construction, and if vulnerabilities



Fig. 3. Partial collapse of parking structure in Northridge, California.



Fig. 4. Partial collapse of parking structure in Glendale, California.



Fig. 5. Structural walls remained uncracked while precast concrete elements collapsed in parking structure in Northridge, California.

were identified, to make recommendations to improve the performance of these structural systems in future seismic events. During the first phase of the study, detailed analyses of individual precast concrete parking structures were performed to evaluate their response during the Northridge earthquake.^{7,8}

These analyses focused on the role of the diaphragms within the lateral-force-resisting system. Inconsistencies between the observed behavior of the parking structures and the expected behavior of members designed in accordance with the 1989 ACI Building Code⁹ and the 1991 Uniform Building Code¹⁰ were identified. Diaphragms were considered to be vulnerable to earthquake damage because the topping slabs were bonded to the surface of the precast floor members. While it is necessary for the topping slab and precast floor members to act together to resist gravity loads, this composite action had an unintended influence on the response of the diaphragm when subjected to lateral forces.

The cracking patterns that developed within the topping slab diaphragms differed considerably from those expected in monolithic reinforced concrete diaphragms. Therefore, accepted procedures for calculating the capacity of reinforced concrete diaphragms were determined to be inappropriate for topping slab diaphragms and composite topping slab diaphragms. These vulnerabilities had not been identified previously, and were not addressed in

the building codes in use at the time of the Northridge earthquake.^{9,10}

In order to investigate if these vulnerabilities were unique to the individual buildings studied or representative of systemic problems in precast construction, a series of idealized buildings was evaluated. The structural characteristics of these idealized buildings were selected to represent a composite view of precast construction in the Los Angeles, California area. The results of the parametric study confirmed that diaphragms in precast concrete parking structures were susceptible to the

types of damage observed after the 1994 Northridge earthquake.

Changes incorporated into the 1999 ACI Building Code¹¹ based on the results of this parametric study are summarized at the end of this paper. Additional changes related to the selection of chord reinforcement in diaphragms were included in the 1997 Uniform Building Code,¹² and are discussed elsewhere.¹³

STRUCTURAL CHARACTERISTICS OF PARKING STRUCTURES IN EPICENTRAL REGION

Because there are no national specifications addressing structural details in precast concrete structures, construction practices vary considerably throughout the United States. The observed damage to precast parking structures in the epicentral region is linked to the structural details used in the structures. Therefore, the observed structural characteristics of parking structures in the epicentral region are summarized in this section. The details discussed in this section are not necessarily representative of precast construction in other regions of the country.

The precast parking structures in

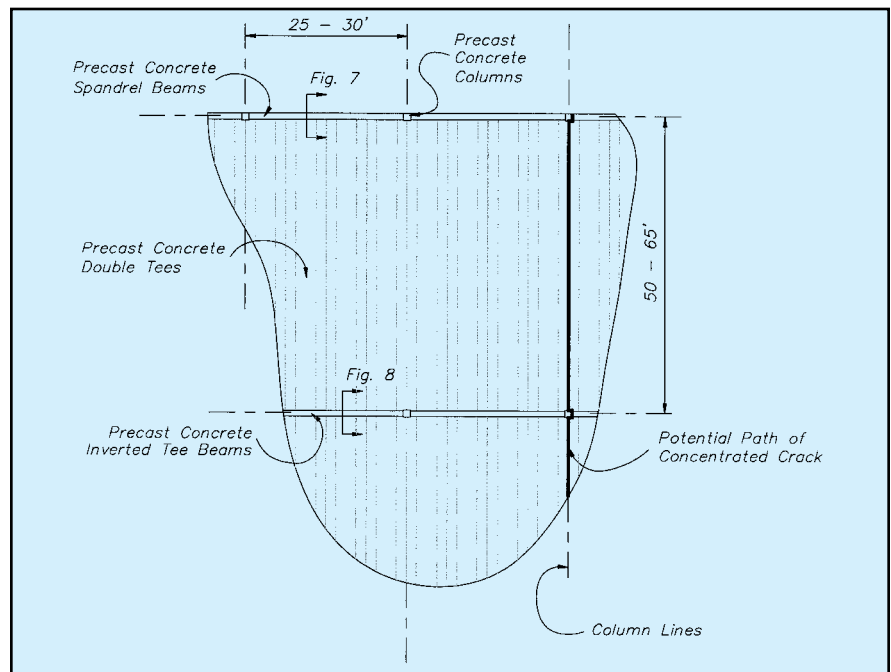


Fig. 6. Typical layout of precast concrete members in parking structures in epicentral region.

Southern California at the time of the Northridge earthquake tended to be short, typically two to four stories in height, and rectangular in plan. Lateral loads were resisted by cast-in-place structural walls. Building owners often require that the number of structural walls be minimized because assailants have found structural walls to be convenient screens when stalking victims. As a result, many parking structures were constructed with two to four structural walls in each direction, and the walls were often located along the perimeter of the building.

Precast members formed the gravity-load-resisting system and were not considered to contribute to the lateral-load resistance of the structures. All precast beams were simply supported and the ends rested on neoprene or korolath bearing pads. As shown in Fig. 6, inverted-tee and spandrel beams were supported on column corbels and had typical spans of 25 to 30 ft (7.62 to 9.14 m).

Double tees were supported on the beam ledges (see Figs. 7 and 8) with typical spans varying between 50 and 65 ft (15.2 to 19.8 m). The columns were typically attached to the foundation through an embedded steel base plate with four, 1 in. (25 mm) diameter bolts. They, therefore, had limited rotational resistance at the base.

Cast-in-place topping slabs, typically 2½ to 3½ in. (65 to 90 mm) thick, covered the precast members and also served as the diaphragms in the lateral-force-resisting system. Unlike many other regions of the United States, the cast-in-place topping slab provided the only connection between the flanges of adjacent double tees. Welded flange connections were not observed in the epicentral region.

The topping slabs were reinforced with welded wire fabric, typically W2.9 x W2.9 with a 6 in. (150 mm) spacing in both directions. Diaphragm chord reinforcement was placed on top of the flanges of the double tees and embedded within the topping slab (see Fig. 7). Un-tensioned strands were used as the chord reinforcement in some structures, while reinforcing bars were used in others.

The specified slab thickness was

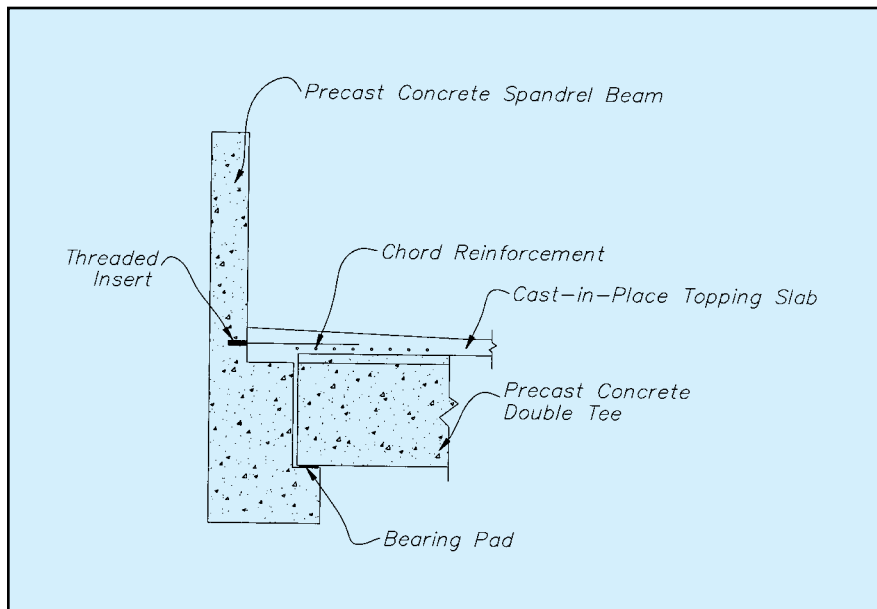


Fig. 7. Typical connection between precast concrete double tee and spandrel beams.

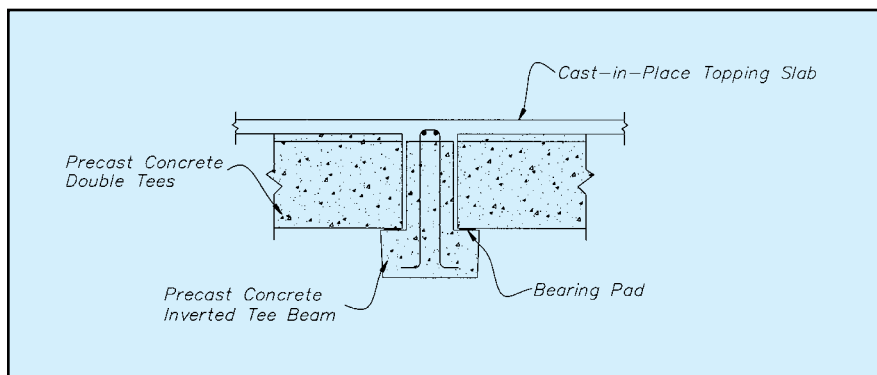


Fig. 8. Typical connection between precast concrete double tee and inverted tee beams.

typically increased in the vicinity of the diaphragm chords to accommodate the added reinforcement. In some cases, a curb was cast above the topping slab and the chord reinforcement was located within the curb. However, the chord reinforcement was typically not confined by transverse reinforcement.

Additional reinforcing bars were placed within the topping slabs along the walls and drag struts to facilitate transfer of inertial forces from the diaphragms into the walls. These Grade 40 bars were typically oriented 45 degrees from the axes of the building, anchored in the walls, and bent into place after the precast members had been positioned.

A variety of details were used to provide a positive connection between the topping slab and the precast mem-

bers. Hooked reinforcing bars were used in some cases to connect the ledger and spandrel beams to the slab, while bars were threaded into inserts in other buildings (see Fig. 7). Stirrups in the inverted tee beams typically extended into the slab (see Fig. 8).

PARAMETRIC STUDY

In order to demonstrate that diaphragms in precast concrete parking structures designed in accordance with the governing building codes^{9,10} at the time of the Northridge earthquake could be vulnerable to earthquake damage, a series of idealized buildings encompassing a wide range of diaphragm lengths and aspect ratios was studied (see Table 1). The assumed dimensions and construction details were representative of actual structures

Table 1. Design forces for structures considered in parametric study.

Overall width (ft)	Overall length (ft)	Aspect ratio	Total weight (kips)	V_b (kips)	V_u (kips)	M_u (kip-ft)
110	150	1.36	4,950	955	318	11,900
	180	1.64	5,940	1145	382	17,200
	210	1.91	6,930	1335	445	23,400
	240	2.18	7,920	1525	509	30,500
	270	2.45	8,910	1720	573	38,700
	300	2.73	9,900	1910	636	47,700
	330	3.00	10,900	2100	700	57,800
165	180	1.09	8,910	1820	573	25,700
	210	1.27	10,400	2005	668	35,000
	240	1.45	11,900	2290	764	45,800
	270	1.64	13,400	2575	859	58,000
	300	1.82	14,900	2865	955	71,600
	330	2.00	16,300	3150	1050	86,600
220	240	1.09	15,800	3055	1018	61,000
	270	1.23	17,800	3435	1145	77,300
	300	1.36	19,800	3820	1273	95,500
	330	1.50	21,800	4200	1400	11,550

V_b = factored design base shear.

V_u = factored design shear at end of roof diaphragm.

M_u = factored design moment at midspan of roof diaphragm.

Note: 1 ft = 0.3048 m; 1 kip = 4.448 kN; 1 kip-ft = 1.356 kN-m.

in the epicentral region; however, a prototype structure did not exist.

A sketch of an idealized parking structure is shown in Fig. 9. Two structural walls constituted the vertical members of the lateral-force-resisting system in each direction. The walls were placed along the perimeter of the structure so that the span of the diaphragm and the dimensions of the structure were the same.

The overall building dimensions were based on the functional requirements of actual parking structures. Transverse and longitudinal bay widths were assumed to be 55 and 30 ft (16.7 and 9.14 m), respectively. The minimum width of 110 ft (33.5 m) corresponds to two transverse bays, and the maximum length of 330 ft (100 m) approximates the largest dimension possible without expansion joints. The building aspect ratios ranged between 1.1 and 3.0, which was consistent with typical construction in Southern California.

All structures were assumed to have two stories with equal heights of 10 ft (3.05 m). Although other researchers have found that the ramps in parking structures act as bracing elements and can influence the distribution of lateral displacements over the height of the building,¹⁴ the ramps were ignored in

this analysis. The vulnerabilities discussed in this paper do not depend on the presence of the ramps.

Design Forces in Diaphragms

It is possible to estimate the design lateral forces in the diaphragms without conducting a detailed structural analysis of each building considered in the parametric study. A number of simplifying assumptions must be made about the distribution of inertial

forces among the structural walls and diaphragms, however. Actual design forces are likely to be different from the idealized values used in this preliminary analysis, but the differences are assumed to have only a minor impact on the conclusions of this study.

The seismic vulnerabilities identified in the detailed analyses of specific buildings were sensitive to the layout of the precast elements.⁷ Therefore, only the transverse seismic response of the idealized structures was consid-

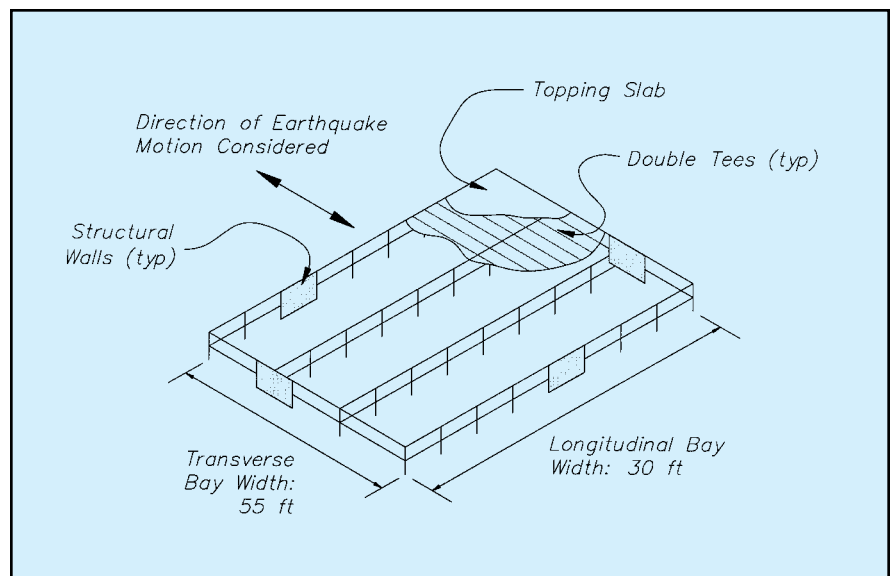


Fig. 9. Idealized precast concrete structures used for parametric study.

ered in this investigation in order to represent the worst case scenario (see Fig. 9).

The equivalent lateral force procedures in the 1991 Uniform Building Code were used to determine the design base shear, V_b , and the distribution of inertial forces over the height of the structure:¹⁰

$$V_b = \frac{ZIC}{R_w} W \quad (1)$$

where

$$C = \frac{1.2S}{T^{2/3}} \leq 2.75 \quad (2)$$

The idealized structures were assumed to be located in Seismic Zone 4 ($Z = 0.4$), and an Importance Factor, I , of 1.0 was used. The R_w factor was assumed to be 8.

The R_w assumption is consistent with typical practice in Southern California, despite the relatively low aspect ratios of typical structural walls in low-rise parking structures. Because the stiffness of the walls was high and the structures were short, the upper limit of 2.75 specified in Eq. (2) was used for C . The seismic dead load, W , was calculated using an average weight of 150 psf (7.2 kPa).

The design base shear specified by Eq. (1) corresponds to $0.138W$ for working loads. The factored design base shear was determined from the load combinations specified in ACI 318-89:⁹

$$U = 0.75 [1.4D + 1.7L + 1.7(1.1E)] \quad (3)$$

$$U = 0.9D = 1.3(1.1E) \quad (4)$$

where

D = unfactored dead load

L = unfactored live load

E = unfactored earthquake load

The governing factored base shear was determined using Eq. (3) to be $0.193W$. The factored base shear is plotted as a function of the plan dimensions of the buildings in Fig. 10. Because the seismic dead load per unit area was assumed to be constant, the factored base shear increases linearly with the length of the diaphragm for a

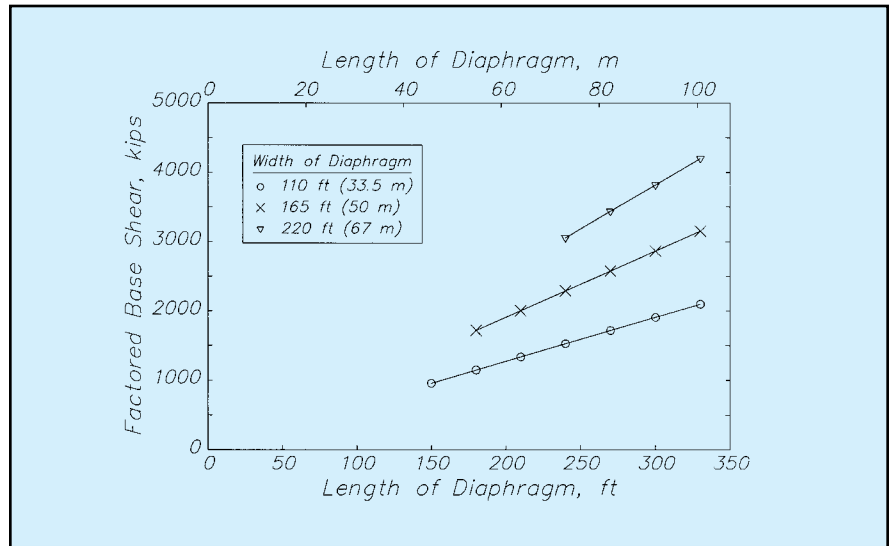


Fig. 10. Variation of design base shear with plan dimensions of idealized precast structures.

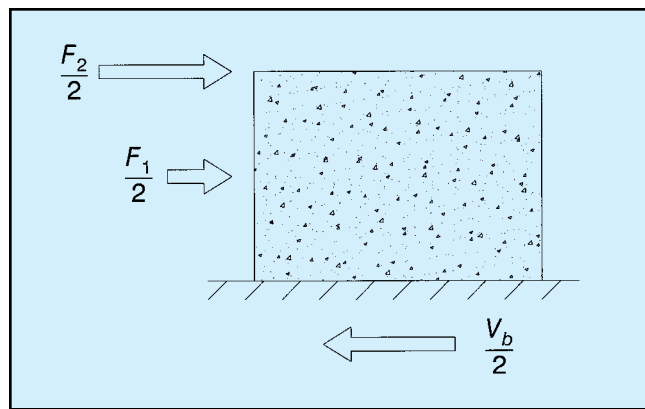


Fig. 11. Assumed distribution of inertial forces to each structural wall.

given width of the building. The factored base shear was assumed to be distributed equally to the two walls in the transverse direction (see Fig. 11).

In accordance with the equivalent lateral force design procedure, the magnitudes of the inertial story forces, F_1 and F_2 , were assumed to increase linearly with height above the base (see Fig. 11).

Detailed analyses of individual parking structures^{7,8} indicated that this assumption was not valid due to the flexibility of the diaphragms. The calculated story inertial forces were nearly uniformly distributed over the height of the buildings. However, the objective of this study was to identify vulnerabilities in buildings designed using the governing building codes.

Therefore, the standard design assumptions were used and the design lateral force at the roof level was assumed to be twice as large as the design lateral

force at the first elevated level.

Each diaphragm was idealized as a simply supported beam and the inertial forces were assumed to be uniformly distributed along the length (see Fig. 12). The maximum shear force occurs at the end of the diaphragm and is equal to:

$$V_u = \frac{w_u \ell^2}{2} = \frac{F_i}{2} \quad (5)$$

The maximum moment occurs at midspan of the diaphragm and is equal to:

$$M_u = \frac{w_u \ell^2}{8} = \frac{F_i \ell}{8} \quad (6)$$

where

w_u = equivalent, uniformly distributed, inertial load

ℓ = length of diaphragm

F_i = story inertial force at level i

i = story level; 1 for first elevated

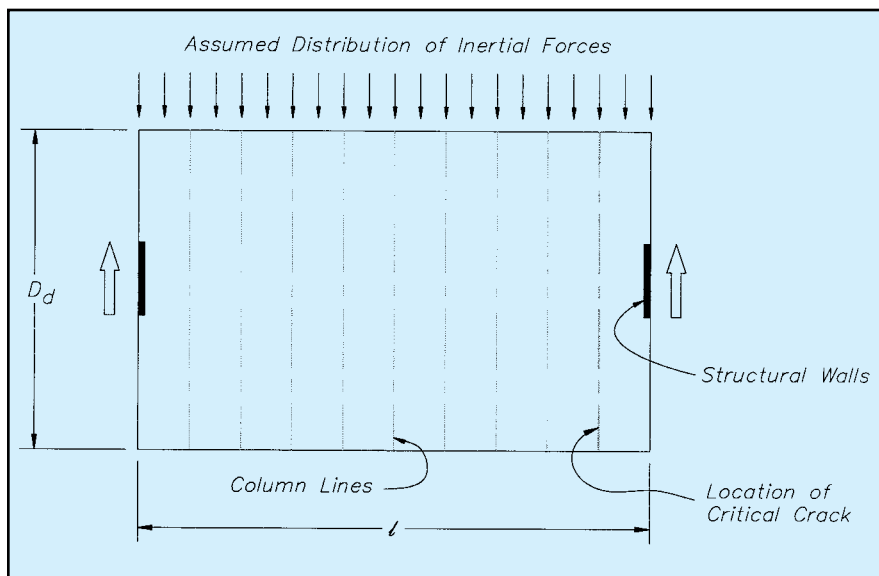


Fig. 12. Assumed distribution of inertial forces in roof diaphragm.

level and 2 for roof

Because the design inertial forces at the roof are higher than those at the first elevated level, the maximum design forces in the diaphragm will occur at the roof level. Factored moments and shears in the roof diaphragms are summarized in Table 1 for the buildings considered in the parametric study.

Selection of Reinforcement in Diaphragms

Reinforcement in the diaphragms was selected using the provisions of Chapter 21 of ACI 318-89.⁹ Chord reinforcement is typically concentrated near the edges of the diaphragm, and distributed reinforcement is positioned in both longitudinal and transverse directions throughout the web (see Fig.-13).

The nominal shear strength of a structural diaphragm depends on the net area of the cross section, A_{cv} , and the transverse reinforcement ratio, ρ_n .⁹

$$V_n = (2\sqrt{f'_c} + \rho_n f_y) A_{cv} \quad (7)$$

The net area was interpreted to be the width of the diaphragm times the thickness of the topping slab. The flanges of the double tees that formed the floor system were not considered to be part of the diaphragm.

A topping slab thickness of 3 in. (76 mm) was used for all diaphragms. The compressive strength of the concrete, f'_c , was assumed to be 4000 psi

(28 MPa). Welded wire fabric was used as the distributed reinforcement in the topping slabs; therefore, the yield stress of the web reinforcement, f_y , was assumed to be 70,000 psi (480 MPa).

The web reinforcement was selected by setting the nominal shear strength defined in Eq. (7) equal to the factored design shear at the end of the diaphragm, defined in Eq. (5), divided by a strength reduction factor of 0.85 for shear.

Because the effective areas of the diaphragms were so large, the design shear stresses were relatively low. Design shear stresses increased linearly

with the length of the diaphragm, as shown in Fig. 14. For diaphragms less than 200 ft (60 m) in length, the contribution of the concrete to the nominal shear strength exceeds the shear demand.

As shown in Fig. 15, the reinforcement ratio needed to satisfy the strength criterion given in Eq. (7) was less than the required area of temperature and shrinkage reinforcement for all diaphragms considered. As specified in ACI 318-89, the required area of temperature and shrinkage reinforcement, A_s , in slabs where the yield stress of the web reinforcement exceeds 60,000 psi (410 MPa) is:⁹

$$A_s > \frac{0.0018 \times 60,000}{f_y} bh \quad (8)$$

The depth of the slab, h , used to compute the minimum amount of steel was taken to be the depth of the topping slab alone.

The ratio of the shear capacity of the diaphragms divided by the demand is shown in Fig. 16. This ratio was between 1 and 2.5 for all of the diaphragms considered. The results of these analyses are consistent with observed amounts of web reinforcement in topping slabs in the epicentral region. Modest web reinforcement ratios satisfy the strength and serviceability requirements for topping slab diaphragms in ACI 318-89.⁹

The chord reinforcement in the dia-

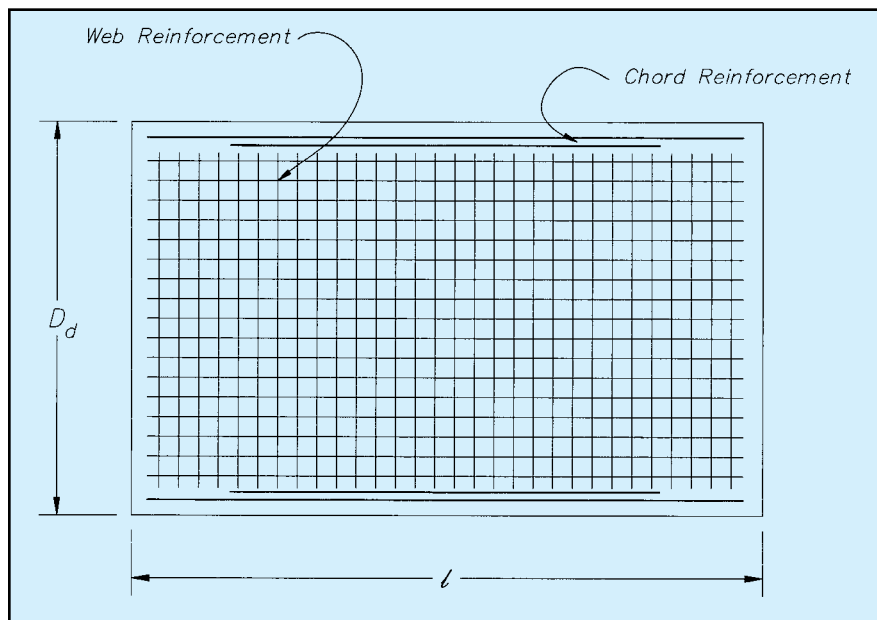


Fig. 13. Assumed layout of reinforcement in diaphragms.

phragm was selected to resist the maximum factored moment at midspan of the diaphragm, defined in Eq. (6), divided by a strength reduction factor of 0.9 for flexure.

The flexural capacity provided by the chord reinforcement may be approximated as:⁹

$$M_n = A_{ch} f_y D_d \quad (9)$$

where

A_{ch} = area of chord reinforcement on one side of diaphragm

f_y = yield stress of chord reinforcement

D_d = width of diaphragm

Because reinforcing bars were commonly used as the chord reinforcement, the yield stress was assumed to be 60,000 psi (410 MPa). The required area of chord reinforcement is plotted as a function of the diaphragm length in Fig. 17.

Additional longitudinal reinforcement was distributed throughout the web to satisfy the temperature and shrinkage reinforcement requirements given in Eq. (8). These minimum reinforcement requirements were developed for out-of-plane bending of slabs, rather than in-plane bending of diaphragms. However, the building codes^{9,10} provide no other guidance for distributed reinforcement in diaphragms.

The selected reinforcement is summarized in Table 2, and the quantities are similar to amounts of reinforcement found in precast concrete parking structures in the epicentral region. The distributed reinforcement ratios tended to be low; however, the area of steel in the web is significant due to the size of the diaphragms.

EVALUATION OF DESIGN PROCEDURE

Following the Northridge earthquake, inconsistencies between the expected and observed behavior of the diaphragms were apparent. Of primary concern to this investigation were the patterns of cracks that developed in the diaphragms. As shown in Figs. 2 and 6, the observed cracks in the topping slab tended to form over the joints between adjacent double tees. The design provisions are based on

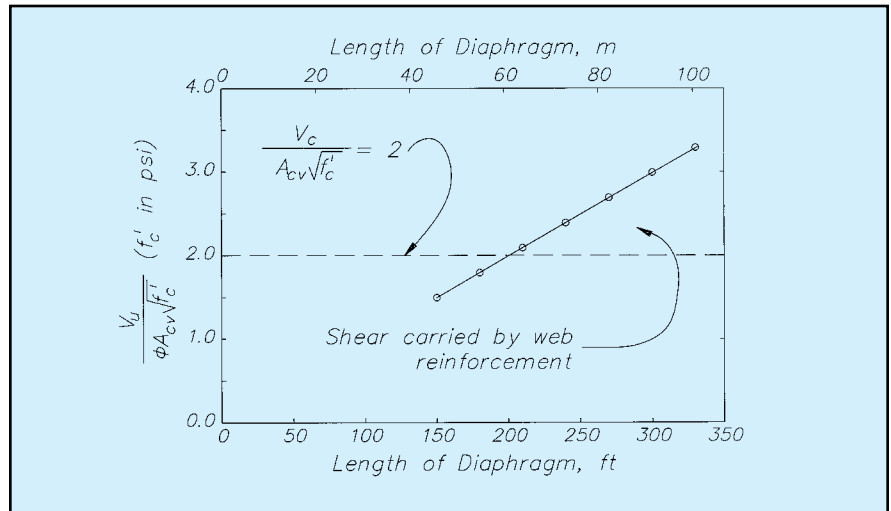


Fig. 14. Average shear stresses at end of diaphragms.

Note: $2\sqrt{f'_c}$ (psi) = $\frac{1}{6}\sqrt{f'_c}$ (MPa)

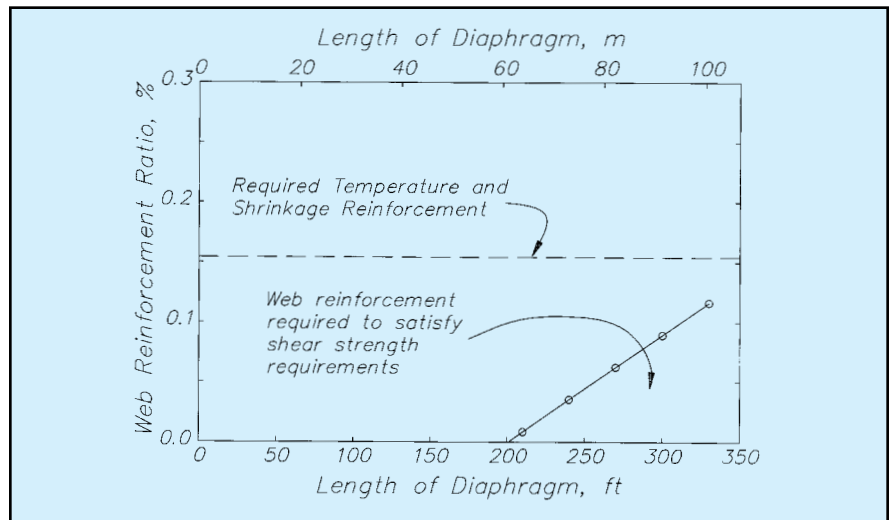


Fig. 15. Required area of web reinforcement in 3 in. (76 mm) topping slab diaphragms calculated using ACI 318-89 procedures.

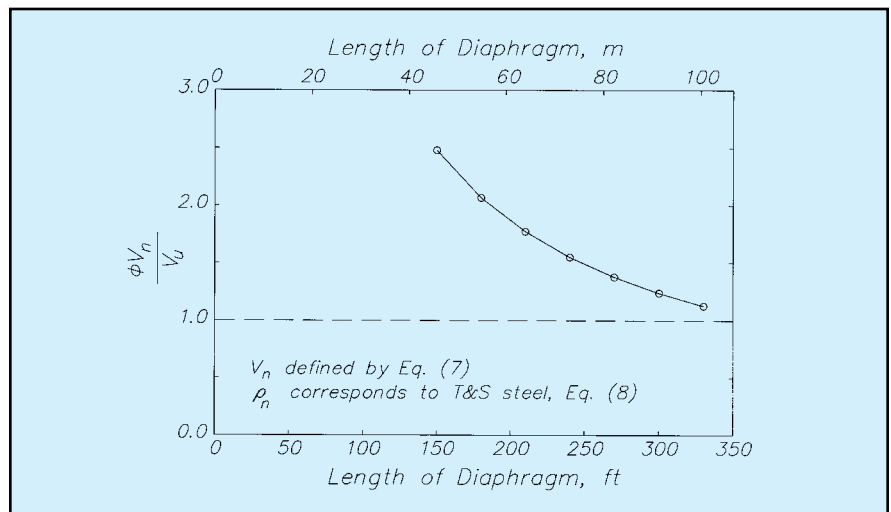


Fig. 16. Ratio of nominal shear capacity calculated using ACI 318-89 procedures to design shear at end of diaphragm.

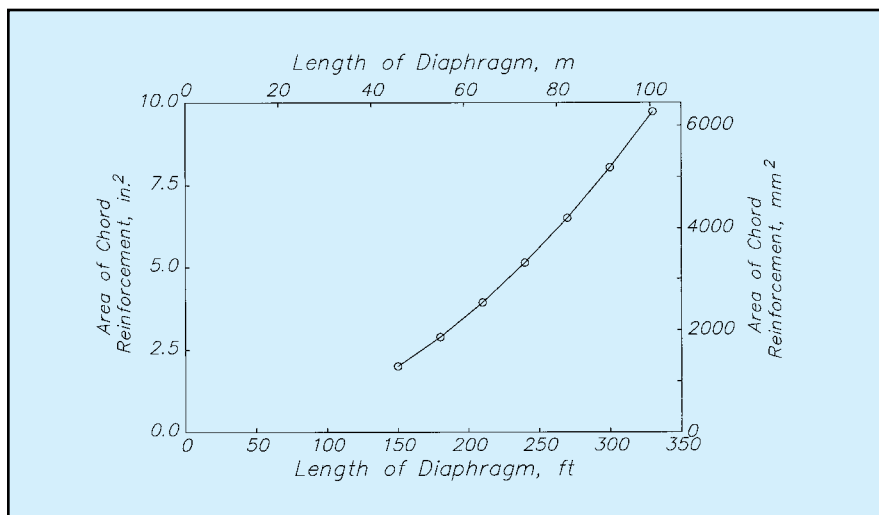


Fig. 17. Required area of chord reinforcement in diaphragm calculated using ACI 318-89 procedures.

the formation of a completely different pattern of cracks; therefore, the calculated nominal shear strength of a topping slab diaphragm may not be representative of the actual capacity.

The design provisions in ACI 318-89 for determining the nominal shear strength of diaphragms, Eq.-(7), were based on the same principles as those for determining the nominal shear strength of reinforced concrete beams. The nominal shear strength of a beam, V_n , is defined as the sum of two components:⁹

(10)

$$V_n = V_c + V_s$$

where V_c is the nominal shear strength provided by the concrete and V_s is the nominal shear strength provided by the transverse reinforcement.

In its simplest form, V_c is defined as:⁹

$$V_c = 2\sqrt{f'_c} b_w d \quad (11)$$

where

b_w = width of web

d = effective depth of tension reinforcement

f'_c = compressive strength of con-

crete in units of psi

The contribution of the steel, V_s , is defined as:⁹

$$V_s = \frac{A_v f_y d}{s} \quad (12)$$

where A_v and s represent the area and spacing of the transverse reinforcement, respectively.

In order to compare the two sets of design equations, a transverse reinforcement ratio, r , is defined as:

$$r = \frac{A_v}{b_w s} \quad (13)$$

which al-

lows the shear strength provided by the transverse reinforcement to be written as:

$$V_s = r f_y b_w d \quad (14)$$

The nominal shear strength of the beam may then be written as:

$$V_n = (2\sqrt{f'_c} + \rho_n f_y) b_w d \quad (15)$$

If ρ_n is substituted for r , and A_{cv} for $b_w d$, then Eq. (15) is identical to Eq. (7).

The significance of the differences between the observed and expected crack patterns is apparent when the ex-

Table 2. Reinforcement in diaphragms selected to satisfy ACI 318-89 provisions.

Overall width (ft)	Overall length (ft)	Web reinforcement ratio (percent)	Total area of web reinforcement (sq in.)	Area of chord reinforcement (sq in.)	ϕV_n Eq. (7) (kips)	ϕV_n Eq. (16) (kips)
110	150	0.154	6.11	2.01	789	487
	180	0.154	6.11	2.89	789	540
	210	0.154	6.11	3.94	789	603
	240	0.154	6.11	5.14	789	675
	270	0.154	6.11	6.51	789	757
	300	0.154	6.11	8.04	789	849
	330	0.154	6.11	9.72	789	950
165	180	0.154	9.16	2.89	1184	723
	210	0.154	9.16	3.94	1184	786
	240	0.154	9.16	5.14	1184	858
	270	0.154	9.16	6.51	1184	940
	300	0.154	9.16	8.04	1184	1032
	330	0.154	9.16	9.72	1184	1133
220	240	0.154	12.22	5.14	1579	1042
	270	0.154	12.22	6.51	1579	1124
	300	0.154	12.22	8.04	1579	1215
	330	0.154	12.22	9.72	1579	1317

Note: 1 ft = 0.3048 m; 1 sq in. = 645 mm²; 1 kip = 4.448 kN.

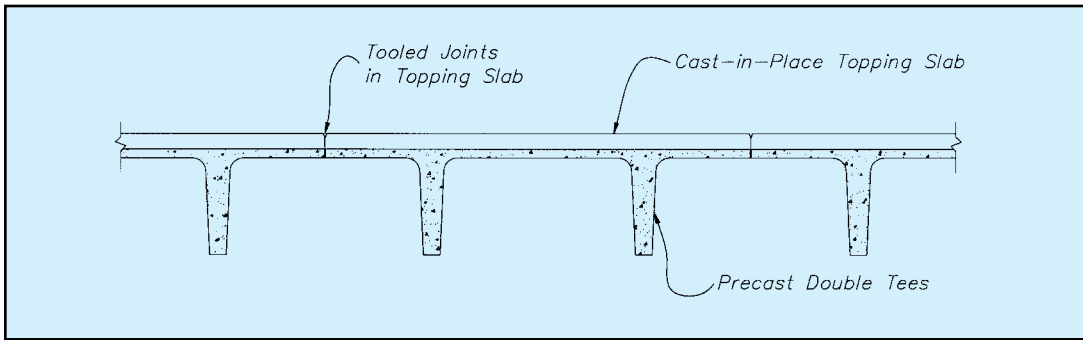


Fig. 18. Typical detail of tooled joints in topping slab.

pected mechanism for developing the nominal shear strength is evaluated. The shear strength provided by the concrete, as defined in Eq. (11), corresponds to “the shear causing significant inclined cracking” of the beam.¹⁵

The transverse reinforcement in beams crosses these cracks and remains essentially unstrained until the inclined cracks have formed.¹⁶ However, inclined cracks did not develop in the diaphragms because the underlying precast members influenced the paths along which the cracks formed in the topping slabs.

In order to develop inclined cracks in the topping slabs, cracks would have had to propagate through the webs of the precast members. This behavior was not observed following the earthquake. Rather, cracks in the topping slab tended to form parallel to the webs of the double tees, as shown in Fig. 2.

In addition to the paths of the cracks being different than expected, the distributed reinforcement in the diaphragm that is positioned perpendicular to the chord reinforcement, which corresponds to transverse reinforcement in a beam, did not cross the cracks that formed in the diaphragm. Therefore, the mechanism for shear resistance in a typical topping slab diaphragm is dramatically different from that in a reinforced concrete beam.

The observed cracks in the diaphragms may be explained by considering the layout of the precast members and standard construction practices. In order to control the locations of shrinkage cracks in the topping slab, joints are often tooled in the slab between the precast double tee panels (see Fig. 18). Therefore, the topping slab is likely to be fully cracked at these locations under nor-

mal service loads.

When inertial forces were induced in the diaphragm during the earthquake, the tooled joints along the column lines tended to open because no cast-in-place or precast elements cross these paths (see Fig. 6). In cases where the webs of a double tee beam straddled a column, cracks were still observed to form along the column line, but they did extend through the flanges of the precast members.⁴

Because the critical cracks in the diaphragm formed along predetermined paths, the shear-friction design method was considered to be a more realistic model for calculating the nominal shear strength of the diaphragm.⁹

$$V_n = A_{vf} f_y \mu \quad (16)$$

where

A_{vf} = total area of steel that crosses crack

μ = coefficient of friction along crack

Because the topping slab is expected

to be cracked along the tooled joints, μ was assumed to be 1.0 for this analysis. As shown in Fig. 13, the longitudinal web reinforcement and the chord reinforcement cross the critical crack, and both were considered to contribute to the shear strength of the diaphragm. ACI 318-89 limits the design yield stress of shear-friction reinforcement to 60,000 psi (410 MPa), so this value was used for both the welded wire fabric and reinforcing bars.

The critical crack was assumed to form one bay from the end of the diaphragm (see Fig. 12). As noted previously, additional reinforcement was typically placed in the topping slab in the vicinity of the walls and drag struts to facilitate transfer of inertial forces. Although the shear demand is highest at the ends of the idealized structures, the capacity of the diaphragms was increased in these regions due to the additional reinforcement. At the location of the assumed critical crack, only the typical distributed reinforcement and a portion of the chord reinforcement is

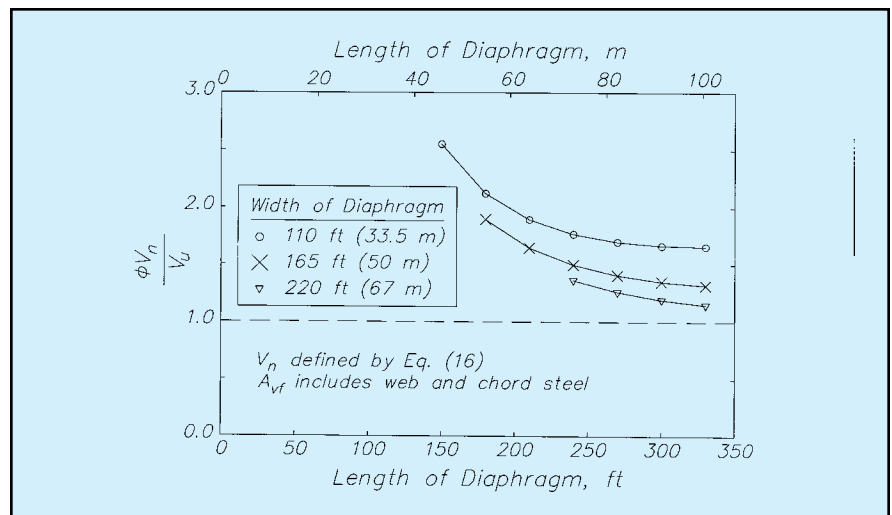


Fig. 19. Ratio of nominal shear capacity calculated using shear-friction model to design shear at location of critical crack.

present in the topping slab.

Because the chord reinforcement was selected to resist the maximum moment at midspan of the diaphragm, one-half of the chord reinforcement at midspan was assumed to be developed at the location of the critical crack. Therefore, the path of the critical crack represented the worst combination of high shear and low reinforcement in the diaphragm.

The ratio of the shear capacity of the diaphragms, calculated using the shear-friction model, divided by the demand at the assumed crack location, is plotted in Fig. 19. Similarly to the ratios calculated using the standard ACI design procedures (Fig. 16), these ratios range from 1 to 2.5 for the diaphragms considered. Therefore, the amount of reinforcement in the topping slab diaphragms selected in accordance with the ACI 318-89 provisions appears to be sufficient to resist the design loads, even if the analytical model used to determine the nominal shear strength of the diaphragms did not represent the observed crack patterns. It should be noted that for all diaphragms considered, the amount of distributed reinforcement was selected to satisfy the temperature and shrinkage requirements for topping slabs.

EXPECTED PERFORMANCE OF IDEALIZED DIAPHRAGMS

The design procedures discussed in the previous sections focus on the strength of the diaphragm. Calculations indicate that when strength is used as the sole criterion, the reinforcement selected in accordance with building code provisions⁹ is sufficient to resist the design lateral forces¹⁰ in the diaphragm. However, the reinforcement must also have the capacity to accommodate the strains that will develop due to the concentrated cracks that form in the diaphragms. Strains are typically not evaluated during the design process.

Iverson and Hawkins² did not report the widths of the cracks that they observed in the parking structure shown in Figs. 1 and 2, but crack widths in the range of 0.1 to 0.2 in. (2 to 5 mm)

are credible based on the photographic evidence. Phillips⁴ reported $\frac{3}{8}$ in. (10 mm) cracks across the entire width of the roof diaphragm in a three-story parking structure, and many $\frac{1}{8}$ in. (3 mm) cracks between adjacent double tees. Therefore, $\frac{1}{8}$ in. (3 mm) was selected as an average width of observed cracks that developed in the topping slabs during the Northridge earthquake, and was used as the basis for all calculations.

Because the wire used to fabricate welded wire fabric is cold drawn, the material is known to be more brittle than the steel used in reinforcing bars. Failure strains have been observed to decrease with decreasing wire size.^{17,18}

Mirza and MacGregor¹⁷ developed the following relationship between the wire size and the mean fracture strain, ϵ_u :

$$\epsilon_u = 0.105 \sqrt{A_n} \quad (17)$$

where A_n is the area of the wire fabric in sq in.

The minimum fracture¹⁷ strain may be obtained by multiplying the strains from Eq. (17) by 0.6 (see Fig.-20).

The impact of the wire material properties on the behavior of the diaphragm may be evaluated by considering the reinforcement in the topping slab that crosses a concentrated crack (see Fig. 21). Because all wires are welded to the perpendicular wires, each wire is anchored at each intersection in the mesh. The strain that develops in the wires crossing the crack is, therefore, equal to the crack width divided by the spacing of the wires:

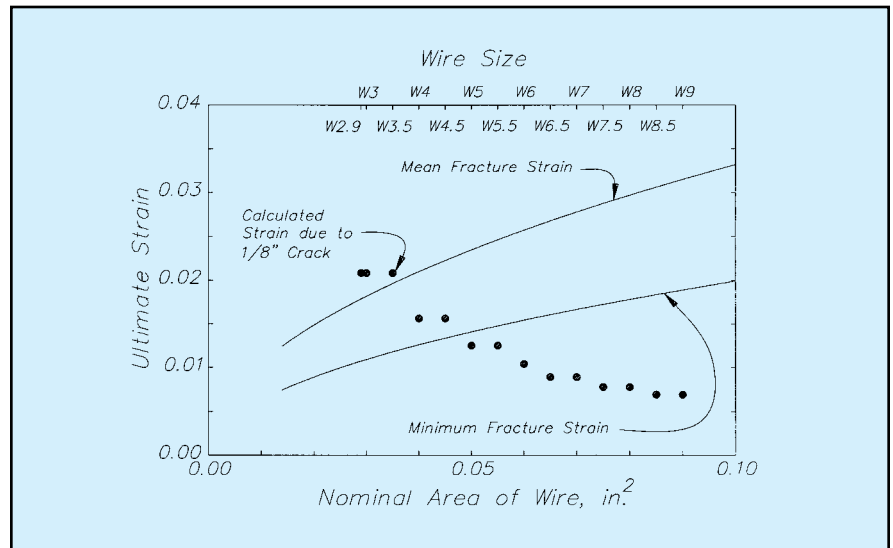


Fig. 20. Variation of fracture strain with wire size (from Mirza and MacGregor¹⁷).

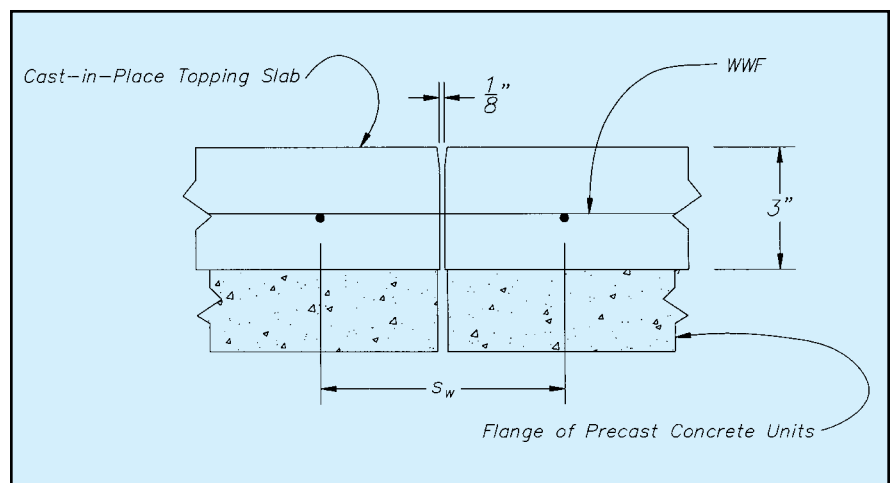


Fig. 21. Detail of topping slab in vicinity of concentrated crack.

$$\varepsilon = \frac{\Delta}{s_w} \quad (18)$$

where

ε = average strain induced in wire crossing crack

Δ = crack width

s_w = spacing of wires running parallel to crack

Average strains in various sizes of wire were calculated assuming a $1/8$ in. (3 mm) crack width, a 3 in. (76 mm) topping slab, and wire spacings selected to satisfy temperature and shrinkage requirements given in Eq. (8). The results are compared with the mean and minimum fracture strains in Fig. 20.

The calculated strains due to the crack exceed the mean fracture strain for wire sizes W3.5 and smaller, and exceed the minimum fracture strain for wire sizes W4.5 and smaller. Therefore, the welded wire fabric commonly used in topping slabs does not have sufficient strain capacity to accommodate the development of a $1/8$ in. (3 mm) crack between adjacent double tees.

As shown in Fig. 22, the welded wire fabric provides a significant portion of the shear strength of the diaphragm. As structural cracks develop in the topping slab during an earthquake, the welded wire fabric crossing the cracks is likely to fracture. The residual shear strength of the diaphragm, which is due to the shear-friction capacity of the chord reinforcement at the location of the critical crack, is considerably less than the capacity of the diaphragm calculated using standard design procedures.

CHANGES TO ACI DESIGN PROVISIONS FOR DIAPHRAGMS

Based on the observed performance of precast concrete parking structures during the 1994 Northridge earthquake, the design provisions for topping slab diaphragms in ACI 318-99 were modified in two ways:

1. The definition of the nominal shear strength has been changed to reflect a mechanism that is consistent with the observed crack patterns.

2. Spacing requirements have been

introduced for welded wire fabric to reduce the likelihood of wire fracture.

The nominal shear strength of a diaphragm comprising a topping slab cast over precast floor elements is now defined as:¹¹

$$V_n = \rho_n f_y A_{cv} \quad (19)$$

where

ρ_n = transverse reinforcement ratio

f_y = yield stress of distributed reinforcement

A_{cv} = net area of cross section

At first glance, the nominal shear strength of topping slab diaphragms in ACI 318-99 appears to be the same as the shear strength provided by the reinforcement in previous codes, i.e., Eq. (7). However, an additional requirement states that web reinforcement must be distributed uniformly in both directions of the diaphragm.

Therefore, Eq. (19) is equivalent to the nominal shear strength provided by the web reinforcement using the shear-friction model, Eq. (16), with a coefficient of friction equal to 1.0. For conservatism, the contribution of the chord reinforcement to the nominal shear strength has been ignored in this formulation.

The amount of distributed reinforcement required by ACI 318-99 for topping slab diaphragms is plotted as a function of the length of the diaphragm in Fig. 23. The maximum

shear demand at the end of the diaphragm was used in this analysis. For the idealized structures studied, the amount of web reinforcement required by Eq. (19) is controlled by the temperature and shrinkage requirements, i.e., Eq. (8), for diaphragm lengths up to 170 ft (51.8 m).

The required amount of web reinforcement exceeds the requirements for temperature and shrinkage reinforcement for longer diaphragms. However, the required amount of web reinforcement is less than two times the temperature and shrinkage requirements for all diaphragms considered.

ACI 318-99 does not specify a minimum reinforcement ratio for shear-friction reinforcement. However, the experimental studies^{19,20} that formed the basis of the shear-friction design provisions indicated that the shear-friction reinforcement will yield following the development of a crack in lightly-reinforced specimens. In these tests, yielding of the reinforcement led to wider crack widths, which reduced the ability of the concrete to transfer shear by aggregate interlock.

In order to avoid this mode of behavior, a minimum value of 150 psi (1 MPa) for $\rho_n f_y$ is recommended for shear-friction reinforcement.^{19,20} This limit is approximately 65 percent higher than the minimum amount of steel needed to satisfy temperature and shrinkage requirements for slabs.

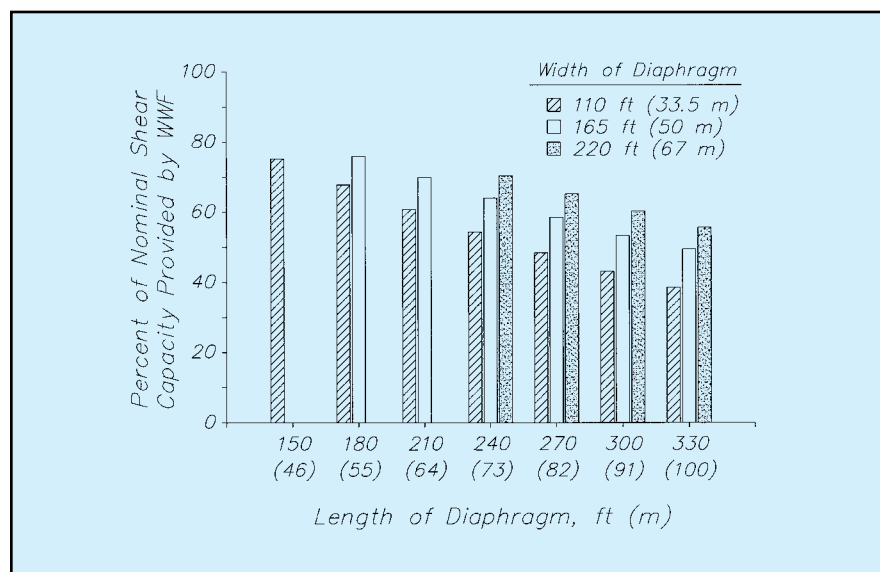


Fig. 22. Nominal shear capacity of diaphragms provided by web reinforcement using shear-friction model [Eq. (16)] and assuming that one-half the maximum chord reinforcement is developed at location of critical crack.

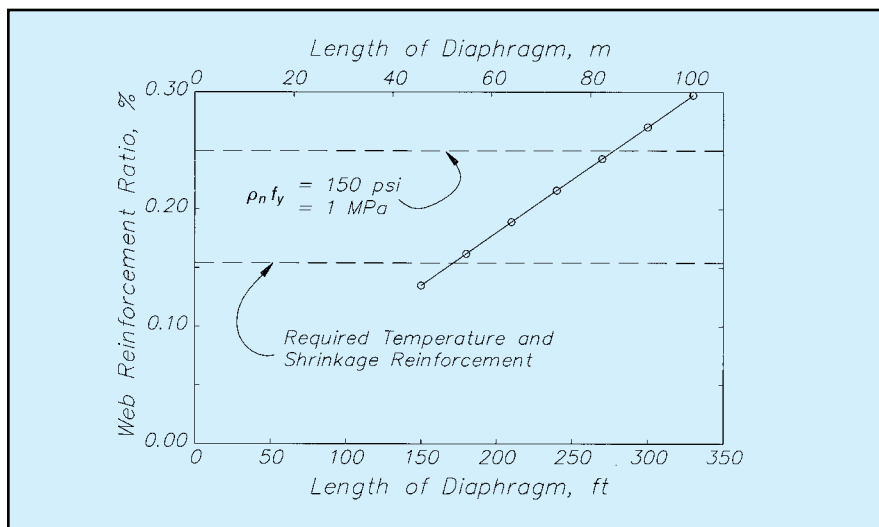


Fig. 23. Required area of web reinforcement in 3 in. (76 mm) topping slab diaphragms calculated using ACI 318-99 procedures.

When welded wire fabric is used for web reinforcement in topping slab diaphragms, a minimum spacing of 10 in. (250 mm) for wires running parallel to the precast members has been introduced. Although indirect, this increased wire spacing is expected to have two beneficial effects on the performance of the diaphragms:

First, the deformations in the wires due to the formation of concentrated cracks will be distributed over a lon-

ger distance, leading to lower average strains in the wires.

Second, designers will select larger wire sizes in order to satisfy the temperature and shrinkage reinforcement requirements, namely, Eq. (8), with the larger wire spacing. Larger wires have larger fracture strains (see Fig. 20).

As indicated in Table 3, a mesh of W5 wires with a spacing of 10 in. (250 mm) satisfies the temperature and shrinkage requirements for a 3 in.

(76 mm) slab, and the average strain induced by a 1/8 in. (3 mm) crack in the topping slab is approximately 50 percent of the mean fracture strain. This is much lower than the strain demand expected for the sizes of welded wire fabric that are currently used in topping slabs.

It should be noted that the maximum spacing for temperature and shrinkage reinforcement in slabs¹¹ of five times the slab thickness or 18 in. (50 mm) must also be satisfied. However, the minimum spacing of 10 in. (250 mm) does not apply for wires running perpendicular to the precast members. Nor does the maximum spacing requirement of two times the slab thickness for flexural reinforcement in critical areas of slabs¹¹ apply to the distributed diaphragm reinforcement.

CONCLUSIONS AND RECOMMENDATIONS

New provisions were introduced into the 1997 Uniform Building Code¹² and 1999 ACI Building Code¹¹ for topping slab diaphragms following the 1994 Northridge earthquake. This paper summarizes the basis for the new requirements in ACI 318-99.¹¹ These provisions address two concerns that were not considered in previous codes:

1. Crack patterns that developed in several precast concrete parking structures in the epicentral region were inconsistent with the mechanism on which previous building code provisions⁹ for diaphragm shear strength were based. The precast floor elements prevented the formation of diagonal cracks in the topping slab diaphragms. Instead, concentrated cracks were observed in the diaphragms along the column lines. These cracks indicated that a shear-friction approach should be used to select the web reinforcement.

2. The closely-spaced welded wire fabric that is typically placed in topping slabs did not have sufficient strain capacity to cross the concentrated cracks. As the critical cracks opened during the earthquake, the welded wire fabric fractured, and the shear strength of the diaphragms was reduced significantly.

Additional measures are also

Table 3. Strains induced in welded wire fabric by 1/8 in. (3 mm) crack.

Wire size	Required spacing* (in.)	Area of steel provided (sq in. per ft)	Strain due to crack	Mean fracture strain	Minimum fracture strain
2.9	6	0.058	0.0208	0.0179	0.0107
3	6	0.060	0.0208	0.0182	0.0109
3.5	6	0.070	0.0208	0.0196	0.0118
4	8	0.060	0.0156	0.0210	0.0126
4.5	8	0.068	0.0156	0.0223	0.0134
5	10	0.060	0.0125	0.0235	0.0141
5.5	10	0.066	0.0125	0.0246	0.0148
6	12	0.060	0.0104	0.0257	0.0154
6.5	14	0.056	0.0089	0.0268	0.0161
7	14	0.060	0.0089	0.0278	0.0167
7.5	16	0.056	0.0078	0.0288	0.0173
8	16	0.060	0.0078	0.0297	0.0178
8.5	18	0.057	0.0069	0.0306	0.0184

*Spacing required to satisfy temperature and shrinkage requirements for 3 in. (76 mm) slab and $f_y = 70,000$ psi (480 MPa).

Note: 1 in. = 25.4 mm; 1 sq in. per ft = 2116 mm²/m.

recommended to minimize the risk of diaphragm damage in future earthquakes:

3. The analyses discussed in this paper have demonstrated that shears and moments induced in the diaphragms during an earthquake increase with the length of the diaphragm. Therefore, reducing the span of the diaphragms by distributing the vertical members of the lateral-force-resisting system throughout the floor plan can reduce the seismic demands on the diaphragms and may provide alternate load paths within the structure.

4. The paths of the concentrated cracks that were observed in damaged diaphragms formed along column lines and did not cross any cast-in-place or precast concrete members. Strategic placement of structural walls or cast-in-place horizontal elements across these potential crack paths may provide resistance to crack growth during an earthquake.

FUTURE RESEARCH

This investigation has also identified a number of specific topics where additional research is needed to reduce the seismic vulnerability of structural concrete construction:

1. Observed damage during the Northridge earthquake provided convincing evidence that structural performance is not always controlled by the inelastic behavior of the vertical members of the lateral-force-resisting system. Yet, building codes typically link the level of the design lateral forces to these elements through the

R_w and R factors.^{10,12} Modifications to these procedures are needed to ensure that the horizontal elements of the lateral-force-resisting system do not yield before the vertical elements, and thereby control the response of the structure. This is particularly important in low-rise buildings, such as the parking structures studied. It is unlikely that squat structural walls will achieve the same ductility levels as slender walls, and the magnitude of the R factors imply that considerable ductility is expected.

2. The empirically-based analytical models used to calculate the shear strength of diaphragms (the modified truss analogy in ACI 318-89 and the shear-friction model in ACI 318-99) were developed from laboratory tests of small-scale specimens. Tests of large beams in Japan²¹ have shown that the average shear stress at failure decreases as the size of the beams increases if the size of the aggregate is held constant. Experimental evidence is needed to confirm that the shear-friction models used for diaphragms, in which the flexural level arm is approximately three orders of magnitude larger than the aggregate, are valid. In addition, the shear-friction model in ACI 318-99 is based on the response of specimens subjected to monotonically increasing loads. Subsequent investigations^{22,23} have shown that the strength and stiffness of specimens subjected to cyclic loading degrade as the number of cycles increases. Experimental evidence is also needed to confirm that the shear-friction model is appropriate for topping slab dia-

phragms that are likely to experience multiple loading cycles during an earthquake.

3. Experimental tests are needed to determine if the minimum reinforcement requirements for out-of-plane bending of slabs are sufficient for in-plane bending of diaphragms, especially in view of the strain concentrations at the joints between adjacent precast concrete members.

ACKNOWLEDGMENTS

The investigation reported in this paper was sponsored by the National Science Foundation, the Precast/Prestressed Concrete Institute, and the Portland Cement Association (PCA R&D Serial No. 2406). The contents of this paper reflect the views of the writers, who are responsible for the technical content. The contents do not necessarily reflect the views of the sponsors.

Andreas V. Quinn and Tim J. Maund, former graduate students at the University of Washington, and Melanie J. P. Townsend, former graduate student at the University of Illinois, performed the detailed analyses of precast concrete parking structures in the epicentral region of Northridge earthquake.

James O. Jirsa, Denis Mitchell, and Todd W. Perbix are thanked for providing photographs of the earthquake damage. Thanks are also extended to the structural engineers and precast concrete producers in Southern California who provided the drawings of specific buildings. Lastly, the writers

wish to express their appreciation to the PCI JOURNAL reviewers for their comments and suggestions.

REFERENCES

1. Corley, W. G. (primary contributor), "Concrete Parking Structures," Northridge Earthquake Reconnaissance Report, V. 2, Earthquake Engineering Research Institute, *Earthquake Spectra*, Supplement C to V. 11, January 1996, pp. 75-98.
2. Iverson, J. K., and Hawkins, N. M., "Performance of Precast/Prestressed Concrete Building Structures During the Northridge Earthquake," PCI JOURNAL, V. 39, No. 2, March-April 1994, pp. 38-55.
3. Phillips, R. J., "Performance of Parking Structures in the Northridge Earthquake," *Proceedings*, 63rd Annual Convention, Structural Engineers Association of California, Lake Tahoe, CA, September 1994, pp. 177-182.
4. Phillips, R. J., "Santa Monica College, Precast Concrete Parking Structure," *1994 Northridge Earthquake — Building Case Studies Project*, Proposition 122, Product 3.2, Seismic Safety Commission, State of California, Sacramento, CA, pp. 137-142.
5. Wood, S. L., Stanton, J. F., and Hawkins, N. M., "Evaluation of Parking Garage Response During the 1994 Northridge Earthquake," *Proceedings*, Eleventh World Conference on Earthquake Engineering, Acapulco, Mexico, June 1996.
6. Wood, S. L., Stanton, J. F., and Hawkins, N. M., "Influence of Floor Diaphragms on the Seismic Response of Precast Parking Garages," *Proceedings*, NEHRP Conference and Workshop on Research on the Northridge, California Earthquake of January 17, 1994, California Universities for Research in Earthquake Engineering, Volume III-A, 1998, pp. 189-196.
7. Quinn, A. V., "Parking Garages in the Northridge Earthquake," Thesis submitted in partial fulfillment of the requirements for the MSCE degree, Department of Civil Engineering, University of Washington, Seattle, WA, 1995.
8. Maund, T. J., "Seismic Behavior of Diaphragms in Parking Garages," Thesis submitted in partial fulfillment of the requirements for the MSCE degree, Department of Civil Engineering, University of Washington, Seattle, WA, 1995.
9. ACI Committee 318, "Building Code Requirements for Reinforced Concrete (ACI 318-89)," American Concrete Institute, Farmington Hills, MI, 1989.
10. *Uniform Building Code*, International Conference of Building Officials, Whittier, CA, 1991.
11. ACI Committee 318, "Building Code Requirements for Reinforced Concrete (ACI 318-99)," American Concrete Institute, Farmington Hills, MI, 1999.
12. *Uniform Building Code*, International Conference of Building Officials, Whittier, CA, 1997.
13. *Analysis of Revisions to the 1997 Uniform Codes*, International Conference of Building Officials, Whittier, CA, 1997.
14. Fleischman, R. B., Sause, R., Pessiki, S., and Rhodes, A. B., "Seismic Behavior of Precast Parking Structure Diaphragms," PCI JOURNAL, V. 43, No. 1, January-February 1998, pp. 38-53.
15. ACI Committee 318, "Commentary to Building Code Requirements for Reinforced Concrete (ACI 318R-89)," American Concrete Institute, Farmington Hills, MI, 1989.
16. ACI-ASCE Committee 326, "Shear and Diagonal Tension," *ACI Journal*, V. 59, No. 1, January 1962, pp. 1-30; No. 2, February 1962, pp. 227-334; and No. 3, March 1962, pp. 352-396.
17. Mirza, S. A., and MacGregor, J. G., "Strength and Ductility of Concrete Slabs Reinforced with Welded Wire Fabric," *ACI Journal*, V. 78, No. 5, September-October 1981, pp. 374-381.
18. Hawkins, N. M., and Hjortset, K., "Minimum Reinforcement Requirements of Concrete Flexural Members," Chapter 15, *Applications of Fracture Mechanics to Reinforced Concrete*, A. Carpenter (Editor), Elsevier, 1991, pp. 379-412.
19. Hofbeck, J. A., Ibrahim, I. O., and Mattock, A. H., "Shear Transfer in Reinforced Concrete," *ACI Journal*, V. 66, No. 2, February 1969, pp. 119-128.
20. Mattock, A. H., and Hawkins, N. M., "Shear Transfer in Reinforced Concrete — Recent Research," PCI JOURNAL, V. 17, No. 2, March-April 1972, pp. 55-75.
21. Shioya, T., Igura, M., Nojiri, Y., Akiyama, H., and Okada, T., "Shear Strength of Large Reinforced Concrete Beams," *Fracture Mechanics: Applications to Concrete*, Special Publication 118, American Concrete Institute, Farmington Hills, MI, 1989.
22. Hawkins, N. M., "Seismic Resistance of Prestressed and Precast Concrete Structures," PCI JOURNAL, V. 22, No. 6, November-December 1977, pp. 80-110.
23. Abdel-Maksoud, M. G., "Relationship Between Performance and Geometric and Mechanical Properties of Concrete Joints Subjected to Cyclic Shear," Thesis submitted in partial fulfillment of the requirements for the PhD degree, Department of Civil Engineering, University of

APPENDIX — NOTATION

<p>A_{ch} = area of chord reinforcement on one side of diaphragm</p> <p>A_{cv} = net area of diaphragm cross section</p> <p>A_n = area of wire</p> <p>A_s = required area of temperature and shrinkage reinforcement, per ACI 318</p> <p>A_v = area of transverse reinforcement</p> <p>A_{vf} = total area of reinforcement that crosses path of predetermined crack</p> <p>b_w = width of web of beam</p> <p>C = factor used to specify design base shear, per 1991 UBC</p> <p>D = dead loads or related internal moments and forces, per ACI 318-89</p> <p>D_d = width of diaphragm and idealized building</p> <p>d = effective depth of longitudinal reinforcement in beam</p> <p>E = load effects of earthquake or related internal moments and forces, per ACI 318-89</p> <p>F_i = factored inertial force at story i</p> <p>f'_c = specified compressive strength of concrete</p> <p>f_y = specified yield stress of reinforcement</p> <p>h = thickness of topping slab</p> <p>I = importance factor, per 1991 UBC</p> <p>i = story level</p> <p>L = live loads or related internal moments and forces, per ACI 318-89</p>	<p>ℓ = span of diaphragm and overall length of idealized building</p> <p>M_n = nominal flexural capacity of diaphragm</p> <p>M_u = factored design moment at midspan of diaphragm</p> <p>R = factor used to specify design base shear, per 1997 UBC</p> <p>R_w = factor used to specify design base shear, per 1991 UBC</p> <p>r = transverse reinforcement ratio in beam</p> <p>S = site coefficient for soil characteristics, per 1991 UBC</p> <p>s = longitudinal spacing of stirrups in beam</p> <p>s_w = spacing of wires running parallel to crack</p> <p>T = fundamental period of building</p> <p>V_b = design base shear, per 1991 UBC</p> <p>V_c = contribution of concrete to nominal shear strength of beam</p> <p>V_n = nominal shear strength of reinforced concrete member</p> <p>V_s = contribution of web reinforcement to nominal shear strength of beam</p> <p>V_u = factored design shear at end of diaphragm</p> <p>W = seismic dead load, per 1991 UBC</p> <p>Z = seismic zone factor, per 1991 UBC</p> <p>Δ = assumed width of crack</p> <p>ϵ = average strain in wire crossing crack</p> <p>ϵ_u = mean fracture strain of wire</p> <p>μ = coefficient of friction along crack</p> <p>ρ_n = transverse reinforcement ratio</p>
--	--